

Characterization of the response of IHEP-IME LGAD with shallow carbon to Gamma Irradiation

Weiye Sun^{a,c} Yunyun Fan^{a,b,1} Mei Zhao^{a,b} Han Cui^{a,c} Chengjun Yu^{a,c} Shuqi Li^{a,c} Yuan Feng^{a,c} Xinhui Huang^{a,c} Zhijun Liang^{a,b,1} Xuewei Jia^{a,c} Wei Wang^{a,b} Tianya Wu^{a,b} Mengzhao Li^{a,b} João Guimarães da Costa^a and Gaobo Xu^d

^a*Institute of High Energy Physics, Chinese Academy of Sciences,
19B Yuquan Road, Shijingshan, Beijing 100049, China*

^b*State Key Laboratory of Particle Detection and Electronics,
Beijing 100049, China*

^c*University of Chinese Academy of Sciences,
19A Yuquan Road, Shijingshan, Beijing 100049, China*

^d*Institute of Microelectronics, Chinese Academy of Sciences,
3 Beitucheng West Road, Chaoyang District, Beijing 100029, China*

E-mail: fanyy@ihep.ac.cn, liangzj@ihep.ac.cn

ABSTRACT: Low Gain Avalanche Detectors (LGAD) for the High-Granularity Timing Detector (HGTD) are crucial in reducing pileups in the High-Luminosity Large Hadron Collider. Numerous studies have been conducted on the bulk irradiation damage of LGADs. However, few studies have been carried out on the surface irradiation damage of LGAD sensors with shallow carbon implantation. In this paper, the IHEP-IME LGADs with shallow carbon implantation were irradiated up to 2 MGy using gamma irradiation to investigate surface damage. Important characteristic parameters, including leakage currents, breakdown voltage (BV), inter-pad resistances, and capacitances, were tested before and after irradiation. The results showed that the leakage current and BV increased after irradiation, whereas overall inter-pad resistance exhibited minimal change and remained above $10^9 \Omega$ before and after irradiation. Capacitance was found to be less than 4.5 pF with a slight decrease in the gain layer depletion voltage (V_{gl}) after irradiation. No parameter affected by the inter-pad separation was observed before and after irradiation. All characteristic parameters meet the requirements of HGTD, and this design can be used to further optimization.

KEYWORDS: Solid state detectors, Radiation-hard detectors, Si microstrip and pad detectors

¹Corresponding author.

Contents

1	Introduction	1
2	IHEP-IME LGAD sensors	2
3	Irradiation and Experiment Setups	3
3.1	Irradiation	3
3.2	Experiment Setups	4
4	Description and Analysis of Result	5
4.1	Leakage Current versus Bias Voltage(I-V)	5
4.2	Inter-pad Resistance versus Bias Voltage	6
4.3	Extra discussion –Capacitance (C-V) and related quantities	7
5	Conclusion	9

1 Introduction

The Phase-II upgrade of the Large Hadron Collider (LHC), known as the High Luminosity LHC (HL-LHC), aims to achieve a luminosity of $5 \times 10^{34} \text{ cm}^{-2}\text{s}^{-1}$, representing a ten-fold increase compared to the LHC[2, 3, 5]. This higher luminosity leads to significant pile-up effects, with an average of approximately 200 events, necessitating the implementation of a High-Granularity Timing Detector (HGTD) in the forward region of the ATLAS detector. The HGTD will incorporate a new type of silicon sensor, the Low Gain Avalanche Detector (LGAD), to enable precise timing measurements of charged tracks and aid in pile-up suppression [1].

LGAD is a type of silicon sensor that offers moderate internal gain, enabling enhanced signal amplitudes and achieving high time and spatial resolutions of better than 20 picoseconds and micrometers, respectively[10, 12, 13]. However, in the high-intensity beam and irradiation environments of the HL-LHC, LGADs are susceptible to various detrimental effects that can significantly impact their lifetime and performance [4, 13, 15]. To ensure the required irradiation hardness, the ATLAS committee has established stringent requirements for the detectors. The LGADs in the HGTD of ATLAS will not be replaced before the completion of half of the data taking of the HL-LHC (2000 fb^{-1}). The anticipated total ionizing dose (TID) irradiation dose for the LGADs is expected to be 1.5 MGy[11].

Multiple institutes, including BNL, FBK, and NDL, have conducted studies on LGADs, investigating the effects of bulk damage caused by irradiation and observing numerous adverse effects on LGAD performance [6, 7, 14]. However, there has been limited research on surface damage specifically related to LGADs with carbon implantation [8]. This study aims to investigate the surface damage induced by gamma-ray irradiation on LGADs with shallow carbon implantation.

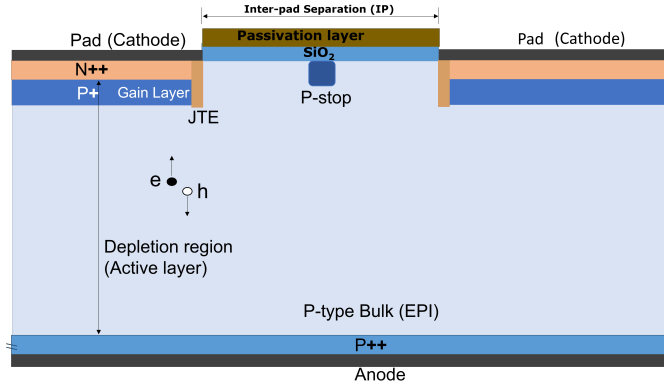


Figure 1: Structure schematic of IHEP-IME LGAD. (Not to scale)

To achieve excellent irradiation hardness, the Institute of High Energy Physics (IHEP) collaborated with the Institute of Microelectronics (IME) to develop a new carbon-doped LGAD named IHEP-IME LGAD. This paper focuses on evaluating the performance of the third version of IHEP-IME LGAD (IHEP-IMEv3 LGAD, or v3) under ^{60}Co gamma-ray irradiation with a maximum dose of 2 MGy. Such irradiation leads to surface damage at the SiO_2 and Si-SiO_2 interface, inducing oxide charges, interface traps, and point defects in the silicon sensors caused by Compton electrons and photoelectrons [9, 16]. The objective of this investigation is to optimize the surface parameters in LGAD design.

This paper is organized as follows: Section 2 presents the v3 LGAD and describes the sample and fabrication process. Section 3 provides details of the irradiation and test setups. The experimental results are presented and analyzed in Section 4, followed by a conclusion in Section 5.

2 IHEP-IME LGAD sensors

LGAD samples used in this study were mainly taken from wafer 12 of v3. Some LGAD samples of the first version of IHEP-IME LGAD (IHEP-IMEv1 LGAD, or v1) were also taken. The structure of v3 from top to bottom is passivation layer, pad, SiO_2 , n^{++} layer, p^+ layer (gain layer), p-type bulk, p^{++} layer and aluminum chuck as illustrated in Figure 1. In comparison to v3, v1 is also shallow carbon-doped LGAD, but it has not undergone surface passivation, which means it does not have the passivation layer shown in Figure 1. From an external perspective, v1 and v3 appear to be identical.

The thickness of p-type bulk is $50\ \mu\text{m}$ and of p^{++} layer is $725\ \mu\text{m}$. A p-stop and JTEs between n^{++} and p^+ layers are designed to reduce the lateral current, and all tested LGADs are quad square pad (2×2 pads, $2\ \text{mm} \times 2\ \text{mm}$ for each pad) structures with different inter-pad separation (IP) from $50\ \mu\text{m}$ to $100\ \mu\text{m}$, surrounded by guard-ring, as summarized in Table 1 and shown in Figure 2. Apart from the difference in IP, all other design parameters of the v3 sample are the same.

The scratches are on the windows of the pads, and the rest is covered by the passivation layer. Since damage to the LGAD caused by ^{60}Co irradiation is mainly concentrated at the SiO_2 surface,

Table 1: Sample and its corresponding IP with irradiation dose. The LGAD of v1 and all six types of IP of v3 were irradiated to three doses, namely 10k, 100k, and 2M Gy.

Sample	Irradiation Dose (Gy)	IP (μm)	Surface Passivation	Shallow Carbon
v3	2-5	10k,100k,2M	Yes	Yes
	2-6	10k,100k,2M	Yes	Yes
	2-7	10k,100k,2M	Yes	Yes
	2-8	10k,100k,2M	Yes	Yes
	2-9	10k,100k,2M	Yes	Yes
	2-10	10k,100k,2M	100	Yes
v1	2-5	10k,100k,2M	No	Yes

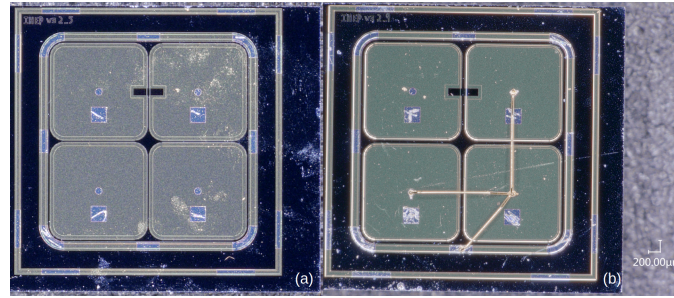


Figure 2: Layout of v3 prototypes 2-5(a) and 2-9(b). Three pads and the guard ring of 2-9 are bonded by gold wires.

different IP designs have different SiO_2 areas, and studying the variation pattern among samples of different IP can help optimize the IP design.

The post-flow test results show that the break-down voltage(BV) of the whole wafer is more than 90% consistent, and therefore, randomly selected samples are representative of the overall situation.

The wafer was uniformly doped with carbon in order to improve the irradiation hardness, and the doping concentration distribution is measured through Secondary Ion Mass Spectrometry (SIMS). Passivation SiO_2 layers are removed before SIMS is performed. The SIMS result is shown in Figure 3. Considering carbon is injected before oxidation and surface passivation, carbon exists in the SiO_2 and passivation layers, but the SIMS does not include these two layers.

3 Irradiation and Experiment Setups

3.1 Irradiation

Irradiation test was carried out at the China Institute of Atomic Energy (CIAE). Samples are fixed using Kapton tapes, and placed in the aluminum boxes, around the cylindrical ^{60}Co irradiation source, which causes damage in silicon sensors by Compton electrons and photoelectrons, as shown in Figure 4. Irradiation dose rate is $1.00 \times 10^4 \pm 15\%$ Gy/h ($2.77 \pm 15\%$ Gy/s). The LGAD of all six types of IP was irradiated to three doses, namely 10k, 100k, and 2M Gy, as summarized in Table 1. Different doses of irradiation for the same IP of LGAD are obtained from different samples from

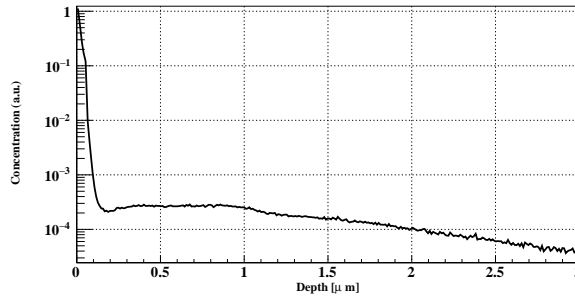


Figure 3: Doping concentration distribution of Carbon, measured through SIMS.



Figure 4: Fixed samples on Kapton tapes (a) are placed in aluminum boxes around the cylindrical irradiation source (b).

Table 2: Errors of experiment apparatus.

Apparatus	Accuracy	Used in measurement
Keithley 2400	0.012%	IV CV Resistance
Keithley 2410	0.02%	IV Resistance
Keysight E4980A	0.05%	CV

the same wafer. Due to the small sample size compared to the diameter of the radiation source, the irradiation is uniform.

3.2 Experiment Setups

All tests, including IV, CV, and Inter-pad resistance, were conducted in the clean room of IHEP at a temperature of 20-22 °C and a humidity of 10-12%. The errors of the measuring apparatus are summarized in Table 2.

The leakage currents are measured from 10^{-13} A to 10^{-4} A, and break-down current is defined as $1 \mu\text{A}$. Negative bias potential is applied to chuck in 2V increment for IV and inter-pad resistances, and in 0.5V increment for CV.

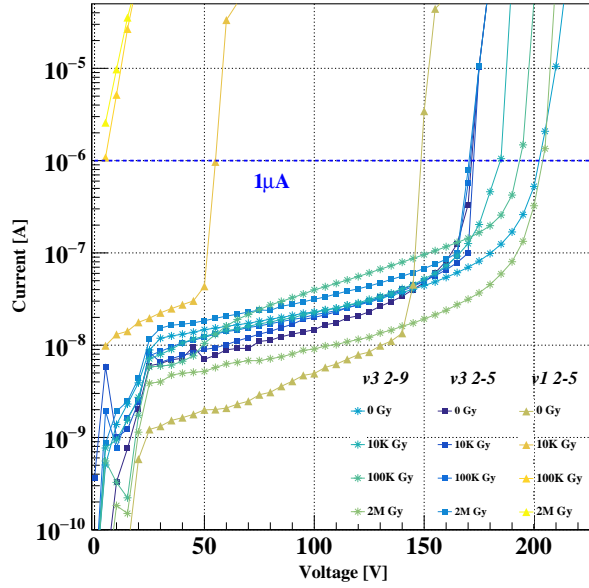


Figure 5: IV characteristic of v3 2-5, 2-9 and v1 2-5.

For IV and CV tests, one pad and guard ring are grounded, with the rest pads floating. For inter-pad resistance, three pads and the guard ring are connected by gold wires and grounded, as illustrated in Figure 2 (b). The rest pad (bias pad) is biased with a voltage range of -1 V to 1 V in 0.5 V increments. The leakage current is measured on ground pads and the bias current is measured on the biased pad.

Since different experiments require different wiring methods, the effects of different wiring methods with respect to the guard ring plus 0, 1, 2, and 3 pads floating are analyzed. No significant change in leakage current and BV are observed by changing the wiring method, and therefore the following experimental results can be excluded as a result of the test method.

4 Description and Analysis of Result

Results of Leakage Current versus Bias Voltage(I-V) and BV are shown in 4.1; inter-pad resistance is analyzed in 4.2; some other issues on bulk damages are discussed in 4.3.

4.1 Leakage Current versus Bias Voltage(I-V)

In general, an increase in both leakage current and BV after irradiation was observed. This conclusion holds for all IP. The following is the detailed analysis process.

I-V characteristics of IHEP-IME LGAD before and after irradiation are measured as shown in Figure 5, and take v3 2-5, 2-9, and v1 2-5 as examples.

For v3 2-5, the leakage currents increase with the rise in irradiation dose, reaching three times the pre-irradiation value after exposure to 2 MGy of irradiation. The variation in breakdown voltage (BV) among different irradiation doses is approximately 5 V. Similarly, for v3 2-9, the trend

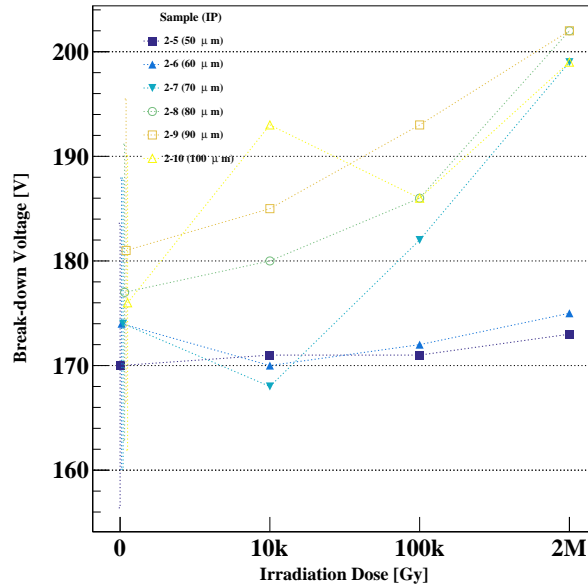


Figure 6: BV of all IP under different irradiation doses. For samples before irradiation, error bars are added according to the spread of BV of the wafer.

of leakage currents before breakdown resembles that of sample v3 2-5, but BV increases by 20 V after being subjected to 2 MGy of irradiation. For v1 2-5, the leakage current is greater than that of v3, and BV is lower than v3 before irradiation. The BV of v1 decreases dramatically after irradiation, indicating that v1 is damaged. v3 samples have undergone a surface passivation process compared to v1, which may be responsible for the increased irradiation hardness but remains to be further investigated. V1 will not be studied in the following due to poor performance.

All samples are investigated in a similar way, and results are shown in Figure 6. BV increases with increasing irradiation dose, rising by 5 V-30 V for different samples after 2M Gy irradiation. This trend is particularly significant in samples 2-7, 2-8, 2-9, and 2-10, where the rise is greater than 20 V. Considering different doses of irradiation for the same IP of LGAD are obtained from different samples from the same wafer and the BV of the whole wafer has about 10% spread before irradiation, a change of 15V or more in BV after irradiation can be deemed to be caused by irradiation. Consequently, the observed BV rise in samples 2-7, 2-8, 2-9, and 2-10 can be attributed confidently to the irradiation effects. The variations observed in 2-5 and 2-6 are smaller than the 10% BV spread, and therefore the relationship between BV and irradiation dose cannot be determined in these cases.

4.2 Inter-pad Resistance versus Bias Voltage

Inter-pad resistance (R) refers to the resistance between electrodes, specifically the resistance between the grounded and biased pads. In operational LGADs, lateral currents can be generated between electrodes, leading to increased noise and reduced signal-to-noise ratio. A larger R-value

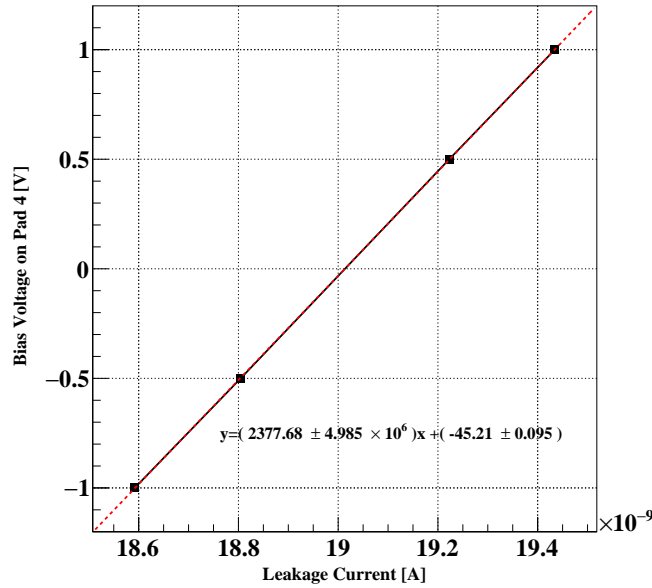


Figure 7: I-V characteristic (solid black line) and linear fit (red dashed line) of v3 2-5 before irradiation at a chuck bias of -85 V.

helps to reduce these lateral currents. In this study, the R values of v3 samples 2-5, 2-6, 2-7, 2-8, 2-9, and 2-10 were measured.

To calculate R, a plot of the bias voltage on the biased pad *vs.* the leakage current is created, and a linear fit is applied to the slope of this I-V characteristic, yielding the resistance value. Figure 7 shows the I-V characteristic and its linear fit for v3 2-5 at a chuck bias of -85 V before irradiation. The plot demonstrates excellent linearity with an R^2 value greater than 0.99. It is worth noting that the current used to calculate R includes the current from both the substrate and neighbor pads. This can result in a lower calculated resistance value, and the actual resistance is higher than the calculated result.

For this study, the reference operating voltage is selected at 85 V. The R of all samples are shown in Figure 8. All samples, including those irradiated to 2 MGy, exhibit R values greater than $10^9 \Omega$, which is two orders of magnitude higher than the non-carbon-doped HPK LGAD irradiated to 2.5 MGy, where R decreases by four orders after irradiation [8]. HPK's LGAD also features a passivation layer. For v3, no significant trends, such as shifts, increases, or decreases in R, were observed, indicating that irradiation did not have a significant impact on R. Since all samples have R values greater than $10^9 \Omega$, it can be concluded that the design of v3 meets the design requirements of having R values greater than 1 G Ω .

4.3 Extra discussion –Capacitance (C-V) and related quantities

This section discusses the capacitance versus bias voltage (CV), V_{gl} , acceptor removal constant. The CVs of v3 2-5 with IP 50 μm are shown in Figure 9. The figure shows the capacitance values

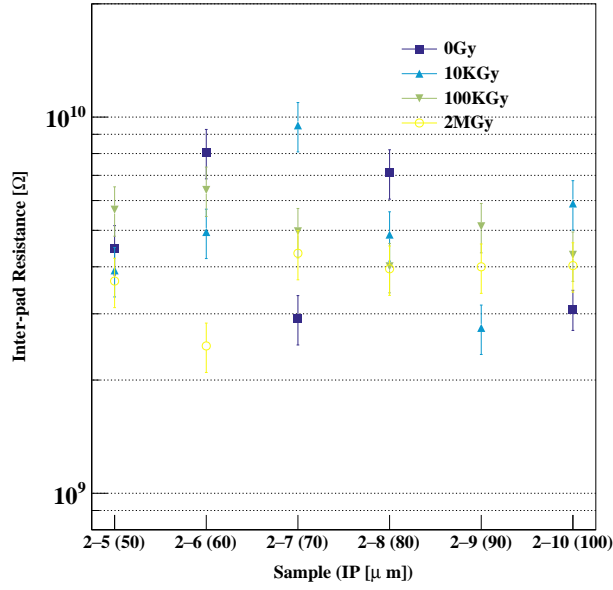


Figure 8: Inter-pad resistance of v3 at chuck bias -85 V of all samples before and after irradiation.

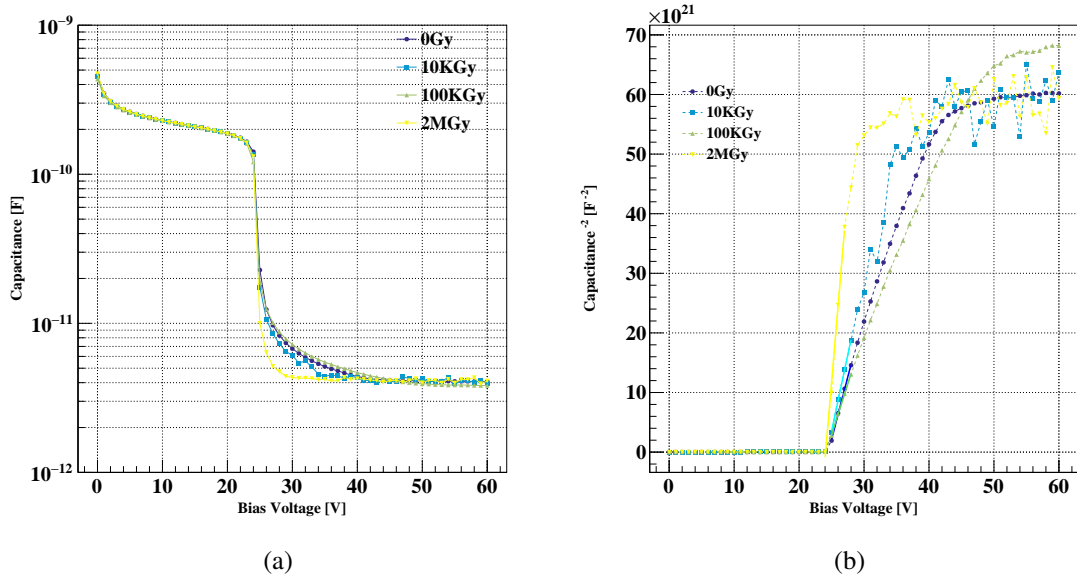


Figure 9: C-V(a) and $\frac{1}{C^2}$ -V (b) characteristics before and after irradiation for v3 2-5 with IP 50 μm . Data are drawn in dashed lines and fittings in solid in (b).

are all less than 4.5 pF, no significant shape change is observed before and after 2M Gy irradiation, and all other samples show the same properties.

Another aspect studied is the gain layer depletion voltage (V_{gl}) and the acceptor removal constant, which characterize the bulk damage effect of irradiation.

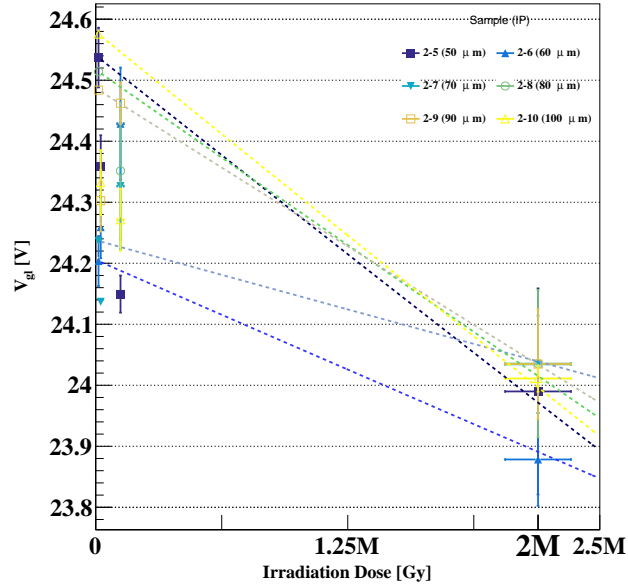


Figure 10: Fitting of gain layer depletion voltage V_{gl} as a function of dose to the function $V_{gl} = V_{0,gl}e^{-c\phi}$ for all samples.

Calculated V_{gl} is the intersection of the linear fitted line through three points after the turning point and the line $y=0$ in the $\frac{1}{C^2}$ -V curve.

Similarly, V_{gl} is calculated for the other samples and fitted to equation (4.1), where V_{gl} and $V_{0,gl}$ represent the gain layer depletion voltages before and after irradiation, ϕ is the total ionizing dose measured in Gy, and c is the acceptor removal constant measured in 1/Gy. The fitting results are presented in Figure 10, and the constants c are determined to be in the order of 10^{-9} for all samples. It can be observed that there is no significant change in V_{gl} across different IP. This suggests that no bulk damage caused by gamma irradiation is observed.

$$V_{gl} = V_{0,gl}e^{-c\phi} \quad (4.1)$$

To summarize, except for the slight decrease in V_{gl} after irradiation, no significant effects of irradiation on other parameters are observed.

5 Conclusion

After ^{60}Co irradiation, the surface components of LGADs were found to be affected, resulting in changes in the studied characteristic parameters. The effects of irradiation on LGADs can be summarized as follows:

- An increase in leakage current by approximately half an order and a small increase in BV were observed after irradiation.

- In the case of v3, no significant change in inter-pad resistance was observed before and after irradiation.
- There was no correlation between the current used to calculate R parameters and inter-pad spacing, and no significant bulk damage was observed in all tests.

Based on these findings, it can be concluded that v3 demonstrates irradiation hardness indicators under the dose of 2M Gy in terms of BV(180-200 V), inter-pad resistance(> 1G Ω), and capacitance(< 4.5 pF). These results indicate carbon doping combined with surface passivation increases radiation hardness. This study will contribute to the optimization of future LGAD surface designs of inter-pad distance, the gap between the active edge and the guard ring, and the maximum fill factor.

Acknowledgments

This work was supported in part by the National Natural Science Foundation of China under Grant 12105298, Grant 12275290 and Grant 12175252; in part by the State Key Laboratory of Particle Detection and Electronics under Grant No.SKLPDE-ZZ-202315.

References

- [1] Technical Proposal: A High-Granularity Timing Detector for the ATLAS Phase-II Upgrade. doi: 10.17181/CERN.CIUJ.KS4H.
- [2] High-Luminosity Large Hadron Collider (HL-LHC) : Preliminary Design Report. 12 2015. doi: 10.5170/CERN-2015-005.
- [3] O Aberle, E Carlier, E Barzi, G Ferlin, C Parente, E Skordis, K Einsweiler, S Atieh, A Patapenka, R Calaga, et al. submitter: High-luminosity large hadron collider (hl-lhc): Technical design report. Technical report, CERN, 2020.
- [4] Shudhashil Bharthuar, Jennifer Ott, Erik Brücken, Akiko Gädda, Stefanie Kirschenmann, Maria Golovleva, and Panja R Luukka. Effect of thermal donors induced in bulk and variation in p-stop dose on the no-gain region width measurements of lgads. In *Proceedings of the 29th International Workshop on Vertex Detectors (VERTEX2020)*, page 010020. Journal of the Physical Society of Japan, jun 2021. doi: 10.7566/jpscp.34.010020.
- [5] Charlotte Cooke. Upgrade of the cms barrel electromagnetic calorimeter for the high luminosity lhc. *Instruments*, 6(3), 2022. ISSN 2410-390X. doi: 10.3390/instruments6030029. URL <https://www.mdpi.com/2410-390X/6/3/29>.
- [6] M. Ferrero, R. Arcidiacono, M. Barozzi, M. Boscardin, N. Cartiglia, G.F. Dalla Betta, Z. Galloway, M. Mandurrino, S. Mazza, G. Paternoster, F. Ficorella, L. Pancheri, H-F W. Sadrozinski, F. Siviero, V. Sola, A. Staiano, A. Seiden, M. Tornago, and Y. Zhao. Radiation resistant lgad design. *Nucl. Instrum. Methods Phys. Res. A: Accel. Spectrom. Detect. Assoc. Equip.*, 919:16–26, 2019. ISSN 0168-9002. doi: <https://doi.org/10.1016/j.nima.2018.11.121>. URL <https://www.sciencedirect.com/science/article/pii/S0168900218317741>.
- [7] R. Heller, C. Madrid, A. Apresyan, W.K. Brooks, W. Chen, G. D’Amen, G. Giacomini, I. Goya, K. Hara, S. Kita, S. Los, A. Molnar, K. Nakamura, C. Peña, C. San Martín, A. Tricoli, T. Ueda, and S. Xie. Characterization of bnl and hpk ac-lgad sensors with a 120 gev proton beam. *J. Instrum.*, 17

- (05):P05001, may 2022. doi: 10.1088/1748-0221/17/05/P05001. URL <https://dx.doi.org/10.1088/1748-0221/17/05/P05001>.
- [8] Martin Hoeferkamp, Alissa Howard, Gregor Kramberger, Sally Seidel, Josef Sorenson, and Adam Yanez. Characterization of low gain avalanche detector prototypes' response to gamma radiation. *Front. Phys.*, page 105, 2022. doi: 10.3389/fphy.2022.838463.
- [9] P. Lecoq. *Scintillation Detectors for Charged Particles and Photons*, pages 45–89. Springer International Publishing, Cham, 2020. ISBN 978-3-030-35318-6. doi: 10.1007/978-3-030-35318-6_3. URL https://doi.org/10.1007/978-3-030-35318-6_3.
- [10] C.H. Li, X. Yang, J.J. Ge, T. Wang, X.X. Zheng, Y.J. Sun, and Y.W. Liu. Performance of lgad sensors with carbon enriched gain layer produced by uisc. *Nucl. Instrum. Methods Phys. Res. A: Accel. Spectrom. Detect. Assoc. Equip.*, 1039:167008, 2022. ISSN 0168-9002. doi: <https://doi.org/10.1016/j.nima.2022.167008>. URL <https://www.sciencedirect.com/science/article/pii/S0168900222004375>.
- [11] Rachid Mazini, ATLAS Collaboration, et al. A high granularity timing detector for the atlas phase-ii upgrade. Technical report, ATL-COM-HGTD-2021-014, 2021. URL <https://cds.cern.ch/record/2777584>.
- [12] N. Moffat, R. Bates, M. Bullough, L. Flores, D. Maneuski, L. Simon, N. Tartoni, F. Doherty, and J. Ashby. Low gain avalanche detectors (lgad) for particle physics and synchrotron applications. *J. Instrum.*, 13(03):C03014, mar 2018. doi: 10.1088/1748-0221/13/03/C03014. URL <https://dx.doi.org/10.1088/1748-0221/13/03/C03014>.
- [13] Michael Moll. Displacement damage in silicon detectors for high energy physics. *IEEE Trans. Nucl. Sci.*, 65(8):1561–1582, 2018. doi: 10.1109/tns.2018.2819506.
- [14] Yuhang Tan, Tao Yang, Suyu Xiao, Kewei Wu, Lei Wang, Yaoqian Li, Zhenwei Liu, Zhijun Liang, Dejun Han, Xingan Zhang, and Xin Shi. Radiation effects on ndl prototype lgad sensors after proton irradiation. *Nucl. Instrum. Methods Phys. Res. A: Accel. Spectrom. Detect. Assoc. Equip.*, 1010:165559, 2021. ISSN 0168-9002. doi: <https://doi.org/10.1016/j.nima.2021.165559>. URL <https://www.sciencedirect.com/science/article/pii/S0168900221005441>.
- [15] Tao Yang, Kewei Wu, Mei Zhao, Xuewei Jia, Yuhang Tan, Suyu Xiao, Kai Liu, Xiyuan Zhang, Congcong Wang, Mengzhao Li, Yunyun Fan, Shuqi Li, Chengjun Yu, Han Cui, Hao Zeng, Mingjie Zhai, Shuiting Xin, Maoqiang Jing, Gangping Yan, Qionghua Zhai, Mingzheng Ding, Gaobo Xu, Huaxiang Yin, Gregor Kramberger, Zhijun Liang, João Guimarães da Costa, and Xin Shi. Leakage current simulations of low gain avalanche diode with improved radiation damage modeling. *Nucl. Instrum. Methods Phys. Res. A: Accel. Spectrom. Detect. Assoc. Equip.*, 1040:167111, 2022. ISSN 0168-9002. doi: <https://doi.org/10.1016/j.nima.2022.167111>. URL <https://www.sciencedirect.com/science/article/pii/S0168900222005083>.
- [16] J Zhang, E Fretwurst, R Klanner, I Pintilie, J Schwandt, and M Turcato. Investigation of x-ray induced radiation damage at the si-sio2 interface of silicon sensors for the european xfel. *J. Instrum.*, 7(12):C12012, dec 2012. doi: 10.1088/1748-0221/7/12/C12012. URL <https://dx.doi.org/10.1088/1748-0221/7/12/C12012>.